A Shock-Induced Pulsed Power Switch Utilizing Electro-Explosion of Exploding Bridge Wire

Cong Xu, Peng Zhu, Qiu Zhang, Zhi Yang, Ke Wang, and Ruiqi Shen

***Abstract*—The pulsed power switch plays an important role in a wide variety of pulsed power applications, such as plasma science and high-pressure-impact studies. This article develops a shock-induced pulsed power switch based on electroexplosion of exploding bridge wire (EBW). The electrical field distribution and electrothermal coupling of EBW are simulated using COMSOL Multiphysics software to assess the rationality of structural parameters. Employing microelectromechanical system technology, the switches are mass-produced with only three steps, improving experimental efficiency and lowering the cost. Electrical tests are conducted at a series of operation voltages varying from 600 to 1800 V, and the results indicated that peak current increases linearly with operation voltage, while delay time and rise time all show a slowly declined trend. A potential conduction mechanism is discussed for better understanding, and switch resistance is described mathematically. Finally, microchip exploding foil initiators are used as a test vehicle to verify the capability of the switch, and ultrafine hexanitrostilbene (HNS-IV) pellets are successfully detonated at 0.15 μF/1300 V after the switch is closed.**

***Index Terms*—Electric breakdown, microelectromechanical devices, plasma arc devices, pulse power system switches, shock waves.**

I. Introduction

THE concept of pulsed power technology was born in the 1940s, and became a reality till J. C. Martin compressed pulse width from $\sim\mu$s to $\sim$ns in the 1960s [1], [2]. A pulsed power system generally consists of capacitor or inductor-based energy storage devices, pulsed power switches, transmission lines, and an objective load. Of particular interest is the pulsed power switch that transfers the energy stored in capacitor banks through transmission lines to the objective load within tens or hundreds of nanoseconds, which determines the output characteristics of pulsed power system, and even success or failure [3]. Therefore, there are several basic requirements on a pulsed power switch, such as rapid closure time and low impendence [4]–[7]. With the development of pulsed power technology, more and more switches have appeared, including vacuum switches, gas switches, oil switches, water switches, magnetic switches, laser-driven switches, photoconductive switches, semiconductor switches, and plasma switches [8]–[15]. It is not difficult to conclude that a switch should be open before closing, since dielectric material is sandwiched between two conductors, and should be closed after the dielectric material is removed or destroyed by external energy, whether photonic, electrical, or mechanical. Vacuum and gas switches still prevail in the pulsed power market, though there are many problems to be solved, such as high cost, requirement of out-gassed materials, and accurate assembly [16]–[17]. Researchers have attempted to planarize gas switches using microelectromechanical system (MEMS) technology, but serious ablation and bad sealing hamper further development [18].

Shock-induced dielectric switches are an effective alternative to vacuum or gas switches. By the 1980s, R. A. Graham had done much work on the shock-induced electrical conductivity of polymers [19]. In 1986, D. D. Richardson invented a fast-turn-ON, low-resistance switch used for slapper detonators; it closes when the Kapton film between two conductors is subjected to high-speed impact of a copper flyer driven by cyclic-$[CH_2N(NO_2)]_3$ (RDX) powders [17]. In 1993, D. G. Tasker studied the electrical conductivity of Kapton film under transverse sweeping detonation waves [20]. In 2009, T. A. Baginski utilized the electroexplosive effect of a Schottky diode to destroy the dielectric film between two electrodes and realize electrical conduction [6]. However, the earlier switches either contain energetic materials or require tedious preparation.

For this article, a kind of polymer film with high dielectric strength is placed between two copper film electrodes to withstand high voltage before switching, as shown in Fig. 1. The top film electrode is etched in a bow tie configuration to form an exploding bridge wire (EBW). Once the switch S (i.e., field effect transistor) between the capacitor C_1 and top electrode closes, the EBW is heated by a small amount of energy stored in capacitor C_1, and undergoes a series of phase changes through solid, liquid, and gas to a plasma state, producing an electro-explosion shockwave to punch the polymer film. Then, local failure occurs in the polymer film, resulting in the discharge of high-voltage capacitor C_2, and thousands of amperes form and oscillate in the capacitor discharge circuit (CDC). Using MEMS techniques, only three steps were needed: two film electrodes can be prepared by magnetic sputtering and ultraviolet lithography, and polymer film can be coated by chemical vapor deposition (CVD). But ahead of this, electrical field distribution

Manuscript received September 3, 2019; revised November 25, 2019 and January 23, 2020; accepted March 7, 2020. Date of publication March 12, 2020; date of current version June 23, 2020. This work was supported by the Natural Science Foundation of Jiangsu Province under Grant BK20151486. Recommended for publication by Associate Editor J. M. Rivas Davila. *(Corresponding author: Peng Zhu.)*

The authors are with the School of Chemical Engineering, Nanjing University of Science and Technology, Nanjing 210094, China (e-mail: congxu@njust.edu.cn; zhupeng@njust.edu.cn; qiuzhang@njust.edu.cn; yangzhi@njust.edu.cn; 117103010448@njust.edu.cn; rqshen@njust.edu.cn).

Color versions of one or more of the figures in this article are available online at http://ieeexplore.ieee.org.

Digital Object Identifier 10.1109/TPEL.2020.2980575

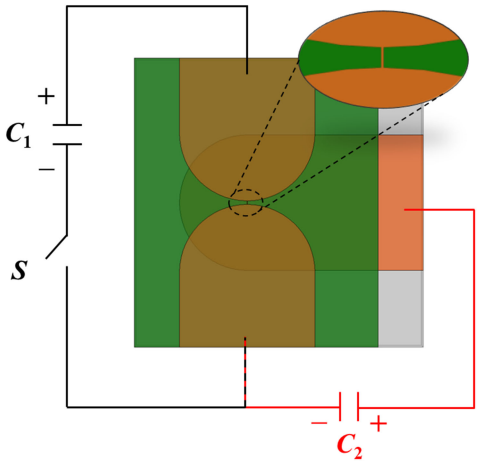

Fig. 1. Schematic representation of pulsed power switch using parylene as insulation layer, as presented in this article.

is simulated by the COMSOL Multiphysics software to assess the dielectric properties of the polymer film, avoiding accidental electrical breakdown before switching. Electrothermal coupling simulation of EBW is performed to analyze the temperature gradient distribution before melting and estimate the energy needed to explode the EBW. Subsequently, electrical tests are conducted to obtain some specific parameters, such as delay time, jitter time, rise time, and peak current, to evaluate the electrical performance. A potential conduction mechanism is then discussed, and a resistance model is established to describe the dynamic switch resistance. Finally, microchip exploding foil initiators (McEFIs) are taken to validate the capability of the switch; whether secondary explosives can be initiated is the most direct proof.

II. Design and Simulation

Due to its excellent characteristics of deposition uniformity, dielectric strength, and survival in harsh surroundings, parylene has been widely used as a coating material [21]. In this article, one of the parylene family, parylene type C with nominal dielectric strength of 220 MV/m, is chosen as the dielectric film sandwiched between two film electrodes. In practice, it withstands less than the theoretical voltage because of inevitable defects in thin film and the influence of electrode shape [22], so it is necessary to predict the electrical field distribution, especially locally, to avoid accidental dielectric breakdowns before switching.

The COMSOL Multiphysics software is used to estimate the electrical field distribution under high voltage. We assume the two film electrodes are each 3.6 μm thick, parylene C is 25 μm thick, and the top electrode is perpendicular to the bottom electrode, as shown in Fig. 1. The relationship between the potential function φ and electrical field $\boldsymbol{E}$ is

$$\boldsymbol{E} = -\nabla\varphi. \tag{1}$$

Combined with Maxwell's equations

$$\nabla \cdot \boldsymbol{D} = \rho \tag{2}$$

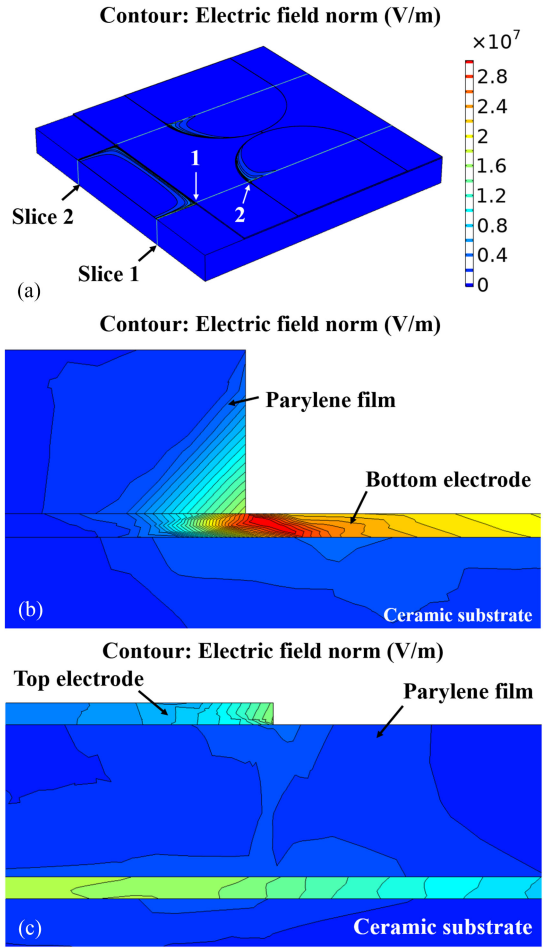

Fig. 2. Electrical field distribution of pulsed power switch under 2000 V. (a) Close-up view. (b) Equipotential lines at point 1. (c) Equipotential lines at point 2.

and

$$\boldsymbol{D} = \varepsilon \boldsymbol{E}. \tag{3}$$

Poisson's equation is derived as

$$-\nabla \cdot (\varepsilon \nabla \varphi) = \rho, \tag{4}$$

where $\boldsymbol{D}$ is the electric displacement, C/m^2; ε is the dielectric constant, C^2/N/m^2; and ρ is the volumetric charge density, C/m^3. A positive voltage of 2000 V is applied on the bottom electrode to obtain an electrical field distribution, as shown in Fig. 2(a). Owing to the symmetry in the switch structure, the electrical field distribution is also symmetric. It is clear that the electrical field mainly concentrates at slices 1 and 2, especially points 1 and 2. In Fig. 2(b), the maximum value occurs at the margin of the parylene C film, about 28 MV/m in the bottom electrode and 6 MV/m in parylene C film, which is much less than 220 MV/m. In Fig. 2(c), the electrical field concentrates at the margin of the top electrode as well as its counterpart area in the bottom electrode, resulting in interior polarization in parylene C film; however, the maximum value is only 3 MV/m. Apparently, the thickness of parylene C is safe enough, even if there exists some internal defects in the thin film.

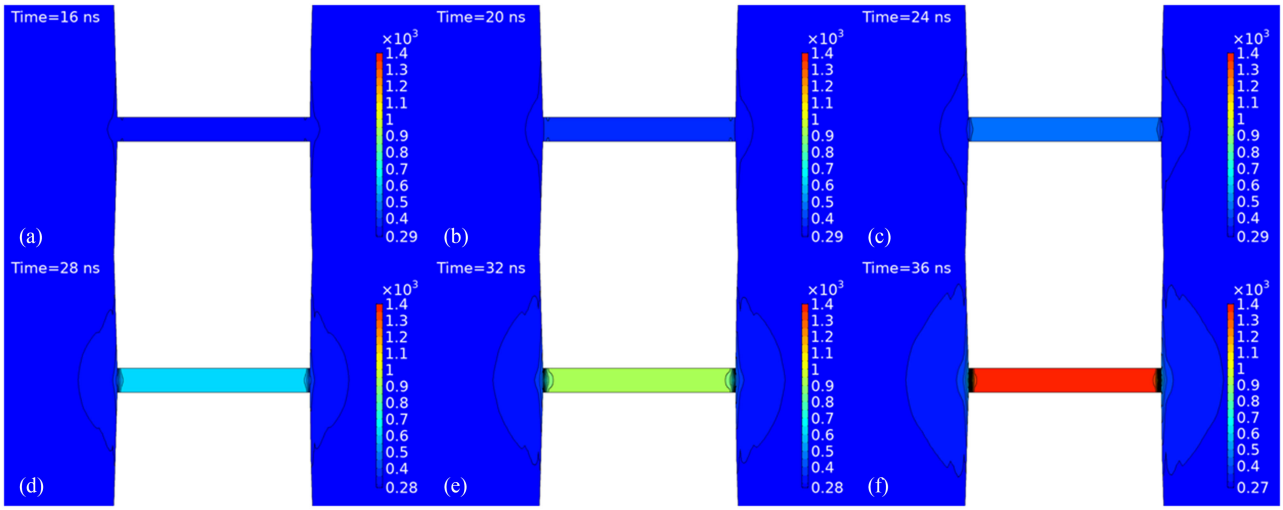

Fig. 3. Electrothermal coupling simulation of EBW of size 80 μm × 10 μm × 2 μm under sine current i(t) = 100 sin(1.57×10^{7}t).

The size of the EBW is also crucial in a pulsed power switch. If the size is large, then the EBW will consume too much energy, bringing some burdens to the trigger circuit. However, a small size generates a smaller shock pressure, which is detrimental to shock the parylene C film. Furthermore, the heating stage before melting has an important effect on the subsequent ionization process. The EBW is expected to be heated uniformly and exploded synchronously. As a result, an electrothermal analysis should be performed in the design stage. Actually, the essence of electrothermal coupling simulation is the solution of the transient heat conduction equation [23]

$$c_v \rho_m \frac{\partial T}{\partial t} = \sigma_e |\boldsymbol{E}|^2 + \nabla \cdot (k \nabla T) \tag{5}$$

where c_v is the heat capacity of the volume of copper, J/kg/K; ρ is the density of copper, kg/m^3; T is the temperature, K; t is the time, s; σ_e is the electrical conductivity, S/m; $\boldsymbol{E}$ is the electrical field, V/m; and k is the heat conductivity, W/m/K. However, the heat capacity, heat conductivity, and electrical conductivity are functions of the temperature, and can be described empirically as

$$c_v = 0.1004T + 355.21 \tag{6}$$

$$k = -0.0685T + 420.75 \tag{7}$$

$$\sigma_e = \left[-4.12 \times 10^{-10} + 0.113 \times 10^{-5} (T/11604)^{1.145}\right]^{-1}. \tag{8}$$

Moreover, the process should be in accordance with the continuity equation of charge transport in the conductor

$$\nabla \cdot \boldsymbol{J} = \boldsymbol{E} \cdot \nabla \sigma_e + \sigma_e \nabla \cdot \boldsymbol{E} = 0 \tag{9}$$

where $\boldsymbol{J}$ is the current density, A/m^2. The length, width, and height of a copper EBW are 80, 10, and 2 μm, respectively. Assuming the current across the EBW rises to 100 A within 100 ns, it can be simplified to a sine curve

$$i(t) = 100 \sin\left(1.57 \times 10^7 t\right). \tag{10}$$

COMSOL Multiphysics was used to obtain the temperature gradient distribution of the EBW before melting. Electrothermal coupling results at different times are shown in Fig. 3. Fig. 3(a) was acquired at t = 16 ns, there is a tiny rise in temperature at this moment. With the continuous injection of current, the global temperature of the EBW rises faster and faster, and reaches the melting point (1358 K) at t = 36 ns, as shown in Fig. 3(f). It should be noted that the areas adjacent to the EBW are also affected. The temperature is highest at the interior and gradually decreases toward the outer regions. In a word, the EBW is heated uniformly, which differs from an exploding bridge foil, whose temperature rise first appears at the corners; this is because the EBW is so slim that the width effect is almost negligible.

III. Experimental Setup

The pulsed power switches were fabricated on 50.8 mm × 50.8 mm ceramic substrate using MEMS technology. Before sputtering the bottom copper electrode, 100 nm of tungsten-titanium layer was overcoated on the substrate. The tungsten was used as an antiablation layer to prevent the copper layer from being ablated by high-temperature plasmas, and the titanium was utilized as an adhesive to bond different components. After the deposition of 3.6 μm of copper, the electrode shape was etched by ultraviolet lithography. Coupling agent was then sprayed on the bottom copper layer to enhance the adhesion force of the polymer film, and 25 μm of parylene C film was coated by CVD, which is an *in situ* preparation technology that contains vaporization, pyrolysis of dimmer, and polymerization of monomer. After that, the top electrode was prepared with same methods as before, and it consists of the following layers: W/Ti-Cu-W/Ti-Au. The gold layer was added to protect the copper layer from oxidation. Fig. 4(a) shows the prepared samples after dicing; 36 switches were obtained at one time. Fig. 4(b) and (c) are photographs showing individual unit and local details of EBW, respectively. Finally, an epoxy pouring sealant was dripped onto the EBW and cured at 65 °C for two hours, as shown in Fig. 4(d),

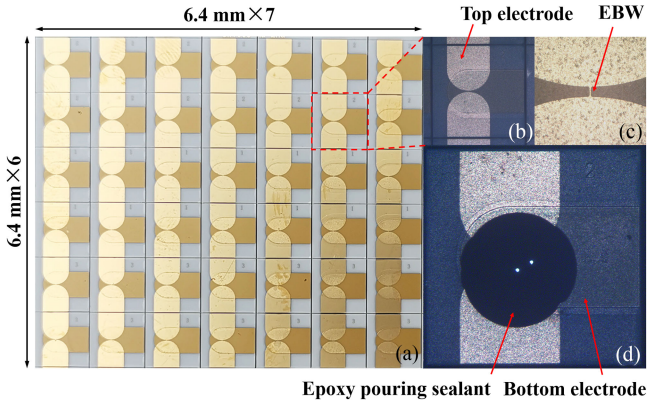

Fig. 4. Photographs of prepared samples. (a) After dicing. (b) Individual unit. (c) Local details of EBW. (d) After encapsulation.

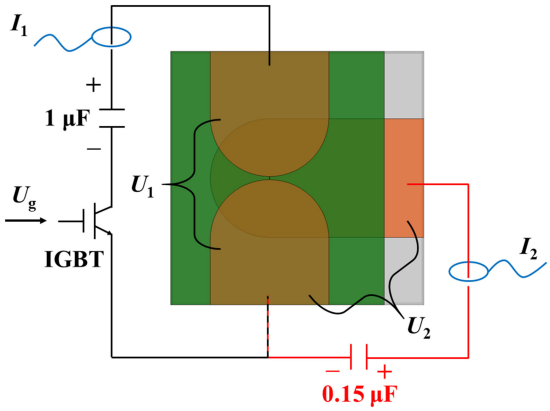

Fig. 5. Schematic representation of the fireset used to characterize the pulsed power switch.

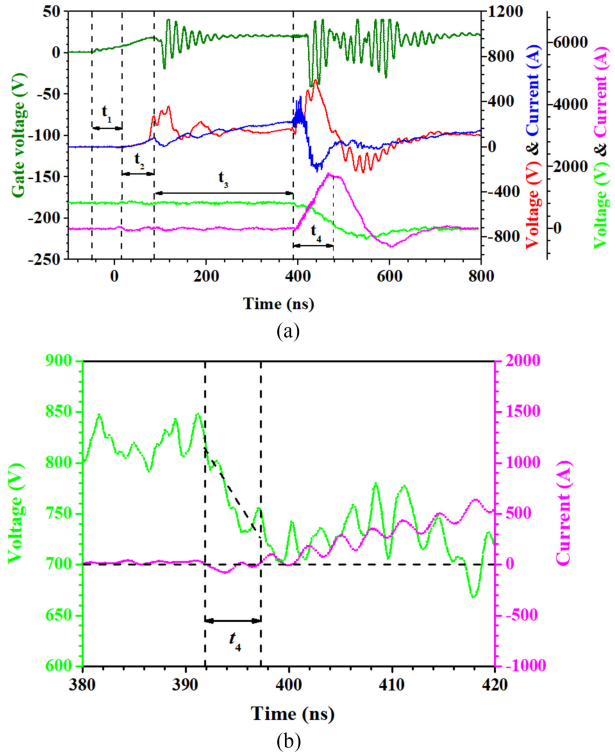

Fig. 6. Electrical curves of pulsed power switch at 0.15 μF/800 V. The dark green line shows the gate voltage of IGBT, the red and blue lines represent the EBW voltage and EBW current, and the green and magenta lines represent the switch voltage and switch current, respectively. (a) Overall curves. (b) Local details.

to better confine the electroexplosion plasma for shocking the parylene C film.

Before detailing experimental measurements, we should make clear which parameters can serve as evaluation criterion to judge whether the switch is good or not. Some parameters often used in vacuum or gas switches, including delay time, jitter time, peak current, and rise time, were applied to quantify the electrical performance of the pulsed power switch [16]. Delay time is often defined as the time from the start of trigger pulse to the start of high-current pulse. An insulated gate bipolar transistor (IGBT), the switch S shown in Fig. 1, was used to control the discharge of capacitor C_1, so the delay time should be counted from the start of gate voltage to IGBT. As every switch exhibits an uncertain delay time, jitter time is used to describe the time difference among the switches, which is a vital indicator of switch stability. Peak current and rise time that are the most important parameters represent the amplitude and width of high-current pulse.

In the experimental setup, two multilayer ceramic capacitors C_1 and C_2 were set to 1 μF and 0.15, respectively, and the switch S was an IXYT80N90C3 type IGBT. The voltage and current signals of interest were captured by high-voltage differential probes and Rogowski coils, respectively, and recorded using a high-speed digital oscilloscope, as shown in Fig. 5.

IV. Results and Discussion

Fig. 6(a) is a typical plot of the firing data of the pulsed power switch operated at 800 V, while the capacitor C_1 is charged to 200 V. The dark green, red, blue, green, and magenta lines represent the gate voltage U_g of the IGBT, EBW voltage U_1, EBW current I_1, switch voltage U_2, and switch current I_2 respectively. The delay time can clearly be divided into four stages. In the first stage, a pathway forms between the emitter and collector electrodes of the IGBT after the gate electrode receives a trigger signal (8 V), which is labeled as t_1, about 63 ns. After 70 ns (labeled as t_2), the EBW voltage U_1 and EBW current I_1 almost peak simultaneously. At this point, the EBW is heated and exploded by the heat induced by the current across it. In the third stage, surplus energy stored in capacitor C_1 is continuously coupled into the copper vapors, leading to ionization of copper atoms and shock pressure of tens of MPa. In the last stage, the parylene C film is broken down under the electro-explosion shockwave, and the switch voltage U_2 drops sharply, as shown in Fig. 6(b). After 7.2 ns (labeled as t_4), the capacitor C_2 begins to discharge, and the switch current I_2 flows through the parylene C film and reaches a maximum value of 1731 A within 64 ns, which is much less than vacuum switches and Baginski's single shot switch (100 ns) [6]. We also found that the switch current I_2 only has one or two oscillation periods, unlike vacuum switches, which can oscillate many times. By solving Kirchhoff's equation, a transient current expression can

be obtained

$$i\left(t\right)=\frac{U_0}{\omega L}\sin\left(\omega t\right)e^{-\beta t} \tag{11}$$

where U_0 is the initial voltage of capacitor C_2, and ω and β, respectively, represent the angular frequency and attenuation coefficient, which are relevant to the inductance L and resistance R of the CDC

$$\omega=\sqrt{\frac{1}{LC}-\frac{R^2}{4L^2}} \tag{12}$$

$$\beta=\frac{R}{2L}. \tag{13}$$

Apparently, the smaller the inductance L, the greater the attenuation coefficient β, and the faster the switch current I_2 returns to zero. By derivation of (11)

$$i'\left(t\right)=\frac{U_0}{\omega L}\left[\omega\cos\left(\omega t\right)e^{-\beta t}-\beta\sin\left(\omega t\right)e^{-\beta t}\right]. \tag{14}$$

When $t=0$, (14) can be simplified as

$$i'\left(0\right)=\frac{U_0}{L} \tag{15}$$

and the inductance L can be estimated as

$$L=\frac{U_0}{i'\left(0\right)}. \tag{16}$$

According to the peak and rise time of the switch current I_2, it can be simplified to a sine expression

$$i\left(t\right)=1731\sin\left(2.45\times10^7t\right). \tag{17}$$

Given the initial voltage (800 V), we calculate the inductance is 18.8 nH.

A series of operation voltages varying from 600 to 1800 V were applied on the capacitor C_2 to study the electrical performance of the switch. Five shots were made at each data point, and the results are plotted in Fig. 7. In Fig. 7(a), the relationship between peak current and operation voltage is almost linear, which means that the switch resistance is constant. When the switch current comes to summit, we know $\sin(\omega t)=1$, then (11) can be simplified as

$$i(t)_{\max}=\frac{U_0}{\omega L}e^{-\beta t}. \tag{18}$$

If the fireset was fixed, the resistance R and inductance L are invariable, and the angular frequency ω and attenuation coefficient β are also invariable. Equation (18) is transformed in

$$i(t)_{\max}=c\cdot U_0 \tag{19}$$

where c is a constant. Fig. 7(b) shows that the delay time decreases slowly as the operation voltage increases, which reveals that the dielectric breakdown is also dominated by the operation voltage. The higher the operation voltage, the higher the polarization. Under the electroexplosion shockwave, it is more prone to dielectric breakdown at higher electrical field. The delay time and rise time also fluctuate up and down with tolerances of tens or hundreds of nanoseconds, perhaps because the ionization process and electrode ablation are unstable.

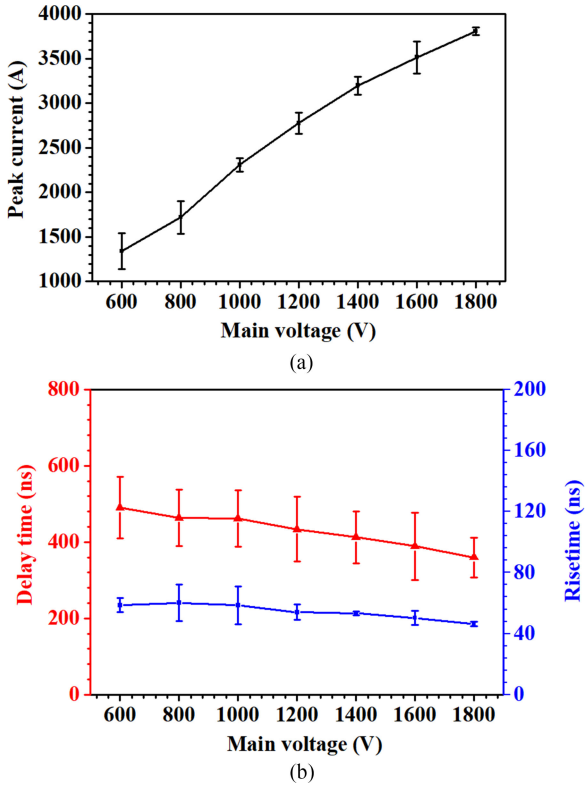

Fig. 7. Peak currents, delay times, and rise times under different operation voltages varying from 600 to 1800 V with a step length of 200 V.

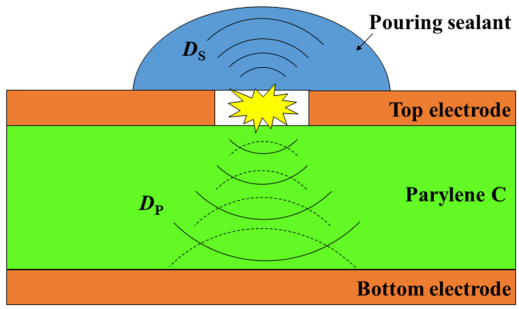

Fig. 8. Illustration of shockwave propagation after the electro-explosion of EBW.

V. Conduction Mechanism and Resistance Model

After the EBW is exploded, electro-explosion shockwaves propagate simultaneously toward the pouring sealant and parylene C film with shock velocities of D_S and D_P, respectively, as depicted in Fig. 8. When the shockwave in parylene C interferes between the parylene C and the bottom electrode, a reflection shockwave generates and propagates in the opposite direction, as the shockwave impedance of copper $(\rho D)_{Cu}$ is higher than that of parylene C. However, the wave impedance of the mixture of copper vapors and plasmas is lower than that of parylene C, and thus a rarefaction wave occurs and unloads the shock pressure when the reflection wave interferes between the parylene C and copper vapors. The duration time of the shock pressure

clearly is

$$t = \frac{2d_P}{D_P} \tag{20}$$

where d_P and D_P are, respectively, the thickness and shock velocity in the parylene C film. We know that the former is at the μm level, and the latter is at the km/s level, so the duration time is several or tens of nanoseconds, which is in accordance with the t_4 in Fig. 6(b). In fact, the switch can be considered as a capacitor before switching, and its capacitance is obtained by

$$C = \frac{\varepsilon S}{4\pi k d}. \tag{21}$$

In physical experiment, it can also be measured by

$$C = \frac{Q}{U}. \tag{22}$$

Using a simple *LCR* meter, the switch capacitance was easily measured as 8.7 pF. The essence of the switching process is the failure of capacitor. Dielectric breakdown mainly includes three basic processes: space charge injection, treeing initiation, and treeing expansion. Space charge generally refers to the trapped charge, that is, the charge that stays in the dielectric after being trapped. Traps can be caused by contamination during production, machining, or application. Treeing breakdown occurs in the detrapping process of trapped charge. When the external environment provides appropriate stimulation to these trapped charges, such as the sudden rise of high electric field, mechanical stress or temperature, the electromechanical energy around the charge will be released rapidly. If the detrapping time of trapped charge is less than the relaxation time of the dielectric, the energy is enough to break the bond of polymer composition. After the initiation of the branch, the space charge will be distributed at the top of the branch through the microchannel network. The electric field at the location of the charge distribution will be greatly enhanced, and the treeing will develop forward. Finally, a plasma channel forms between the two electrodes, and the switch turns on, which allows the high voltage to arc across the two electrodes [6].

D. D. Richardson [24] found that the switch resistance is variable, and developed a dynamic switch resistance model with two assumptions: the switch resistance immediately drops from infinity to some value R_0; and after a certain time t_s passes, the switch resistance drops linearly from R_0 to 0. L. Nappert made corrections: the drop in switch resistance from infinity to R_0 takes some time; and the switch resistance will not reach zero, but rather a constant value (about 0.1 Ω) [25]. For the switch proposed in this article, the drop time from infinity to R_0 can be negligible, since the polarization inside parylene C film is established for an instant once applying high voltage to the two electrodes. When the switch turns ON, the switch resistance drops from R_0 to R_1 linearly in some time t_s. After that, the switch resistance is constant. Therefore, the switch resistance model can be described as

$$\begin{cases} R_s(t) = R_0 \times \frac{t_s - t}{t_s} + R_1, & 0 < t \le t_s \\ R_s(t) = R_1, & t_s < t < t_1 \end{cases} \tag{23}$$

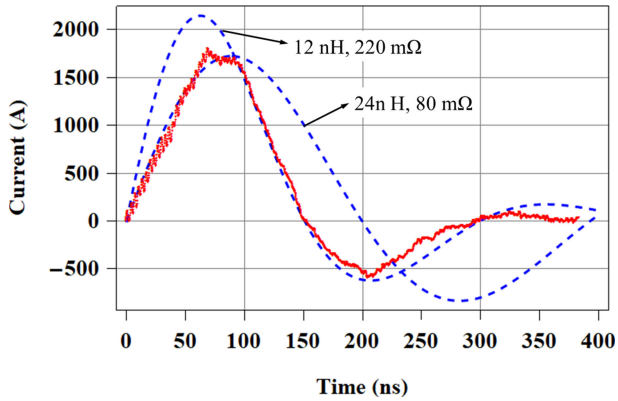

Fig. 9. Comparison between the fitting curves (blue dashed line) and the switch current (red solid line) obtained at 0.15 μF/800 V.

where R_0 and R_1 are, respectively, the resistance before and after switching. In Fig. 6(b), the operation voltage drops linearly from 815 to 698 V within 7.2 ns, and the current still maintains at zero, which means that the switch resistance drops linearly during switching.

As for the switch resistance after switching, we used a mathematical software such as MATHEMATICA to obtain fitting curves. Fig. 9 presents the comparison between the fitting curves and experimental curve obtained at 0.15 μF/800 V. Clearly, the resistance R after switching is not invariable, even including the inductance L. In the first quarter of the first period, the calculated curve fits well with the experimental curve when the resistance R and inductance L are assumed as 80 mΩ and 24 nH, respectively. In the second quarter, the resistance R and inductance L change into 220 mΩ and 12 nH, perhaps due to the ablation uncertainty resulting from the high-temperature plasma arc inside the parylene C film. However, the first quarter is the focus for researchers on pulsed power switch. In a sense, the above resistance model is applicable.

VI. Experimental Validation

An exploding foil initiator (EFI) is an inline flyer-initiating device, consists of a tamper, bridge foil, flyer, barrel, and secondary explosives [26]. When high-current pulse flows through the bridge foil, the narrowest portion will be exploded into plasma to shear out the flyer at the edges of the barrel, and the flyer is then accelerated inside the barrel up to several km/s to impact high explosive, resulting in detonation [27]. With the development of miniature and low-energy EFIs, microchip EFIs (McEFIs) have been prepared with MEMS technology to form a monolithic structure [28]. In this paper, McEFIs were used as a vehicle to validate the capability of the switch. The energy stored in the capacitor is transferred though the switch presented in this document into the bridge foil to drive the plastic flyer to initiate the secondary explosives, as shown in Fig. 10. The McEFIs are made of 3.6-μm-thick bridge foil deposited by magnetron sputtering, 25-μm-thick parylene C flyer coated by CVD, and a 400-μm-thick SU-8 barrel patterned by ultraviolet lithography. The ultrafine hexanitrostilbene (HNS-IV) powders

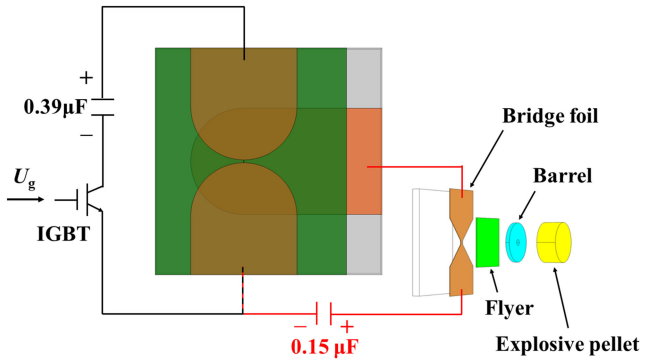

Fig. 10. Schematic representation of the fireset used to function an exploding foil initiator.

were prepared by microfluidic recrystallization [29]. The Bruceton method, also called "up and down," was employed to explore the minimum initiation voltage. Finally, HNS-IV pellets were initiated reliably above 0.15 μF/1300 V.

VII. Conclusion

A sandwich structure pulsed power switch based on the electro-explosion of EBW has been introduced. Employing the multiphysics coupling software, the electrical field distribution and temperature gradient distribution of an EBW were obtained to assess its feasibility and rationality. The results indicated that 25 μm of parylene C film can withstand 2000 V without electrical breakdown, and the EBW can be heated uniformly by a sine current with amplitude of 100 A and rise time of 100 ns. Using MEMS technology, the switches were mass-produced in only three steps, improving experimental efficiency and lowering the cost, which is extremely attractive for low-cost applications and destructive tests. Electrical characterizations were conducted at a series of operation voltages ranging from 600 to 1800 V, with a step length of 200 V. We found that the peak current increases in proportion with the rise of operation voltage, and the delay time and rise time show an insignificant downward trend. The conduction mechanism and dynamic resistance model of the switch were established and discussed, and it was concluded that the switch resistance drops linearly during switching, and is then constant. Finally, McEFIs were utilized to verify the switching capability of the switch. The bridge foil was exploded by pulse current after the switch closed, resulting in flyer acceleration and shock initiation. These results demonstrated the effectiveness of the pulsed power switch.

References

[1] J. C. Martin, "Nanosecond pulse techniques," At. Weapons Res. Establishment, England, Internal Rep. SSWA/JCM/703/27, 1970.
[2] M. Zahn, Y. Ohki, D. B. Fenneman, R. J. Gripshover, and V. H. Gehman, "Dielectric properties of water and water/ethylene glycol mixtures for use in pulsed power system design," *Proc. IEEE*, vol. 74, no. 9, pp. 1182–1221, Sep. 1986.
[3] H. Akiyama *et al.*, "Pulsed power technology," in *Bioelectrics*, Tokyo, Japan: Springer, 2017.
[4] J. V. Parker, R. R. Bartsch, J. C. Cochrane, and S. P. Marsh, "An improved, explosively actuated closing switch for pulsed power applications," in *Proc. IEEE Int. Pulsed Power Conf.*, 1993, pp. 922–925.
[5] T. A. Baginski, R. N. Dean, and E. J. Wild, "Micromachined planar triggered spark gap switch," *IEEE Trans. Compon. Packag. Manuf. Technol.*, vol. 1, no. 9, pp. 1480–1485, Sep. 2011.
[6] T. A. Baginski and K. A. Thomas, "A robust one-shot switch for high-power pulse applications," *IEEE Trans. Power Electron.*, vol. 24, no. 1, pp. 253–259, Jan. 2009.
[7] C. Xu, P. Zhu, K. Chen, W. Zhang, R. Shen, and Y. Ye, "A highly integrated conjoined single shot switch and exploding foil initiator chip based on MEMS technology," *IEEE Electron Device Lett.*, vol. 38, no. 11, pp. 1610–1613, Nov. 2017.
[8] G. J. J. Winands, Z. Liu, A. J. M. Pemen, E. J. M. van Heesch, and K. Yan, "Long lifetime, triggered, spark-gap switch for repetitive pulsed power applications," *Rev. Sci. Instrum.*, vol. 76, 2005, Art. no. 085107.
[9] J. Lv, Q. Zeng, and M. Li. "Metal foil gap switch and its electrical properties," *Rev. Sci. Instrum.*, vol. 84, 2013, Art. no. 045101.
[10] J. N. Nasab, A. Hadizade, S. Mohsenzade, M. Zarghany, and S. Kaboli, "A Marx-based generator with adjustable FWHM using a controllable magnetic switch," *IEEE Trans. Dielectrics. Elect. Insul.*, vol. 26, no. 2, pp. 324–331, Apr. 2019.
[11] G. Denisov, V. Kocharovsky, and M. Kulygin, "Nonlinear nonequilibrium processes in a silicon switch of high-power microwave radiation," *Bull. Rus. Acad. Sci., Phys.*, vol. 73, no. 1, pp. 91–95, 2009.
[12] M. Kulygin, G. Denisov, S. Shubin, S. Salahetdinov, and E. Novikov, "Subterahertz nanosecond switches driven by second-long laser pulses," *IEEE Trans. Terahertz Sci. Tech.*, vol. 7, no. 2, pp. 225–227, Mar. 2017.
[13] T. Jing and C. Zhang, "The model of IGBT as a power switch," in *Proc. Int. Conf. Electron. Commun. Control*, Ningbo, China, Sep. 2011, pp. 1720–1723.
[14] L. Zhang, W. Shi, J. Cao, S. Wang, C. Dong, and L. Yang, "Research on time jitter of gaas photoconductive semiconductor switches in the negative differential mobility region," *IEEE Electron Device Lett.*, vol. 40, no. 2, pp. 291–294, Feb. 2019.
[15] W. C. Nunnally, D. Sanders, S. Sampayan, and G. Caporaso, "High electrical field, high current packaging of SIC photo-switches," in *Proc. IEEE Int. Pulsed Power Conf. Monterey*, CA, United States, Jun. 13–17, 2005.
[16] K. W. Chu and G. L. Scott, "A comparison of high-voltage switches," Sandia Nat. Labs., Albuquerque, NM, USA, Tech. Rep. SAND99-0154, Feb. 1999.
[17] D. D. Richardson and D. A. Jones, "A Fast, low resistance switch for small slapper detonators," Dept. Defence Mater. Res. Lab., Victoria, Australia, Tech. Rep. MRL-R-1030, 1986.
[18] Q. Zhang, C. Xu, P. Zhu, G. Yang, Z. Yang, and R. Shen, "Planar trigger switch and its integrated chip with exploding foil initiator based on low temperature co-fired ceramic," *IEEE Trans. Power Electron.*, vol. 35, no. 3, pp. 2908–2916, Mar. 2020.
[19] R. A. Graham, "Shock-induced electrical switching in polymeric films," in *Mega-Gauss Physics and Technology*, New York, NY, USA: Springer, 1980.
[20] D. G. Tasker, R. J. Lee, and P. K. Gustavon, "An explosively actuated electrical switch using kapton insulation," Naval Surface Warfare Center, Indian Head, MD, USA, Tech. Rep. NSWCDD/Tray/124, 1993.
[21] C. Liu, "Recent developments in polymer MEMS," *Adv. Mater.*, vol. 19, no. 22, pp. 3783–3790, 2010.
[22] J. M. Elizondo-Decanini and E. Dudley, "Pulsed high-voltage breakdown of thin-film parylene C," *IEEE Trans. Plasma Sci.*, vol. 39, no. 11, pp. 3162–3167, Nov. 2011.
[23] S. Jang *et al.*, "Electrothermal analysis of micro/nanowire initiators for energy production applications," Power MEMS, Washington DC, USA, Dec. 1–4, 2009.
[24] D. D. Richardson, "The effect of switch resistance on the ringdown of a slapper detonator fireset," Mater. Res. Lab., Tech Rep. MRL-R-1004, Dec. 1986.
[25] L. Nappert, "An exploding foil initiator system," DREV-R-9502, Mar. 1996.
[26] J. R. Stroud, "A new kind of detonator-the slapper," Lawrence Livermore Lab., Livermore, CA, USA, Tech. Rep. UCRL-7739, 1976.
[27] S. Ebenhöch, S. Nau, and I. Häring, "Validated model-based simulation tool for design optimization of exploding foil initiators," *J. Defense Model. Simul.*, vol. 12, no. 2, pp. 189–207, Apr. 2015.
[28] P. Zhu *et al.*, "Development of a monolithic microchip exploding foil initiator based on low temperature co-fired ceramic," *Sensor Actuat. A, Phys.*, vol. 276, pp. 278–283, 2018.
[29] S. Zhao, J. Wu, P. Zhu, H. Xia, C. Chen, and R. Shen, "A microfluidic platform for preparation and screening of narrow size-distributed nanoscale explosives and super-mixed composite explosives," *Ind. Eng. Chem. Res.*, vol. 57, pp. 13191–13204, 2018.

Cong Xu was born in April 1993. He received the bachelor's degree in 2015 from the Nanjing University of Science and Technology, Nanjing, China, where he is currently working toward the Ph.D. degree with the School of Chemical Engineering.

His research interests include high-voltage switch, electro-explosion of metal, MEMS, and shock loading.

Peng Zhu was born in May 1978. He received the M.S. and Ph.D. degrees from the Nanjing University of Science and Technology, Nanjing, China, in 2007 and 2014, respectively.

He was a Visiting Scholar with Homyel State University, from 2010 to 2011. He is currently an Associate Professor with the School of Chemical Engineering, Nanjing University of Science and Technology. His research activities are focused on PyroMEMS devices, microreactors, and microfluidics.

Qiu Zhang was born in 1993. She received the B.S. degree from the School of Chemical Engineering and Environment from the North University of China, Taiyuan, China, in 2016. She is currently working toward the Ph.D. degree with the Nanjing University of Science and Technology, Nanjing, China.

Her current research interests include design, simulation, and fabrication of the electro-explosive devices, shock loading, MEMS ignition, and detonation system.

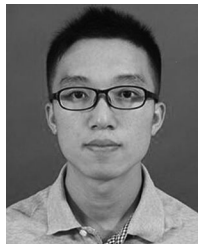

Zhi Yang was born in 1994. He received the B.S. degree in 2016 from the School of Chemical Engineering, Nanjing University of Science and Technology, Nanjing, China, where he is currently working toward the Ph.D. degree.

His research interests include focused on high-speed impact and MEMS devices.

Ke Wang was born in 1995. He received the B.S. degree in 2017 from the School of Chemical Engineering, Nanjing University of Science and Technology, Nanjing, China, where he is currently working toward the Doctorate degree.

His research interests include MEMS ignition and detonation system.

Ruiqi Shen He was born in June 1963. He received the M.S. and Ph.D. degrees from the Nanjing University of Science and Technology, Nanjing, China, in 1986 and 1991, respectively.

He was a Visiting Scholar with the Mendeleyev University of Chemical Technology, Moscow, Russia, from 2001 to 2002. Since 2000, he has been a Professor with the School of Chemical Engineering, Nanjing University of Science and Technology.

His research interests include MEMS devices, microfluidics, nano-energetic materials, laser physics, and chemistry.